Advances in Experimental Medicine and Biology 1097

Bingmei M. Fu · Neil T. Wright *Editors*

Molecular, Cellular, and Tissue Engineering of the Vascular System

Springer

Advances in Experimental Medicine and Biology

Volume 1097

More information about this series at http://www.springer.com/series/5584

Bingmei M. Fu • Neil T. Wright
Editors

Molecular, Cellular, and Tissue Engineering of the Vascular System

Springer

Editors
Bingmei M. Fu
Department of Biomedical Engineering
The City College of the City University
of New York
New York, NY, USA

Neil T. Wright
Department of Mechanical Engineering
Michigan State University
East Lansing, MI, USA

ISSN 0065-2598 ISSN 2214-8019 (electronic)
Advances in Experimental Medicine and Biology
ISBN 978-3-319-96444-7 ISBN 978-3-319-96445-4 (eBook)
https://doi.org/10.1007/978-3-319-96445-4

Library of Congress Control Number: 2018956138

This Springer imprint is published by the registered company Springer Nature Switzerland AG
The registered company address is: Gewerbestrasse 11, 6330 Cham, Switzerland

Preface

Multidisciplinary teams of medical scientists and biomedical engineers, using recent advances in molecular biology, new imaging tools for cell and tissue observations, and modern computational methods and techniques, have made many discoveries and proposed new avenues of exploration in physiology and pathology of mammalian vascular systems. Although these results are routinely presented in the various journals of specific fields, they are seldom systematically introduced to the general audience in the medical and biomedical engineering community. The purpose of this collection is to introduce the recent progress in molecular, cellular, and tissue engineering in the vascular system.

The vascular system is composed of the vessels that carry blood and lymph throughout the body. Arteries, veins, and capillaries circulate blood throughout the body, delivering oxygen and nutrients to the body tissues and removing metabolic waste. This transport function of the vascular system is governed and regulated by the molecular, subcellular, and cellular components forming the vascular wall and the surrounding tissue. Due to its unique location at the interface of the circulating blood and the vascular wall, endothelial surface glycocalyx (ESG) plays important roles as a mechano-sensor and transducer for the blood flow, as a modulator of trans-vascular exchange, and as a barrier to the circulating cells (such as leukocytes) and endothelium adhesion. These roles of ESG are reviewed sequentially in Chaps. 1, 2, and 3. Information received at the vascular surface must be transduced into endothelial cell nucleus for further processing and subsequent use in regulating cellular functions. Chapters 4 and 5 examine the roles of nuclear envelope proteins and nuclear lamina in this process under blood flow-induced shear stress and cyclic stretch. The smooth muscle cells and elastic lamina in the wall of large arteries regulate the blood perfusion rate. Chapter 6 summarizes the regional heterogeneity of these components in the regulation of vasoconstriction in arteries. Following discussion of this basic research, Chaps. 7 and 8 discuss the formation and mechanisms of fibrous cap rupture and vulnerable plaque, and abdominal aortic aneurysm. Chapter 9 presents nonsurgical vascular interventions for coronary artery diseases. After presenting progress in large vessel research, Chap. 10 elucidates the driving force for the movement of red blood cells in narrow capillaries. Chapters 11 and 12 review the experimental studies and mathematical models for tumor metastasis in the microvascular system. Then, Chaps. 13 and 14

discuss transport across a special microvascular wall, the blood-brain barrier, and its role in the clearance of amyloid-β; accumulation of amyloid-β in the brain is one of the factors responsible for Alzheimer's disease. In addition to regulating material transport, our vascular system assists the body temperature control, and the cells of the vascular system also react actively to the temperature change. Chapter 15 reviews the mathematical models of cell response following heating, while Chap. 16 demonstrates applications of hypothermia in enhancing the treatment efficiency in brain and spinal cord injuries. Finally, the biomechanical changes of eardrums to blast waves are described in Chap. 17. Although the eardrum, a multilayer soft tissue membrane, is not in the vascular system, the mechanism for its damage due to the sudden sound pressure may be applicable to the damage of heart valves due to sudden blood pressure changes in the heart.

Last but not least, we sincerely thank our authors for their great contributions to this book. We would also like to thank Dr. Jie Fan, at Rensselaer Polytechnic Institute, and Dr. Yuliya Vengrenyuk, at the Icahn School of Medicine at Mount Sinai, for their help in reviewing some of the chapters in this book. Finally, we would like to thank Ms. Merry Stuber, Editor of Biomedical Engineering at Springer Nature, for her invitation and strong support, and Mr. Sindhuraj Thulasingam, Project Coordinator at Springer Nature, for his tireless assistance. We hope that this book, although covering only limited aspects of the current advances in the vascular system, will bring more collaboration among different disciplines and stimulate more innovative ideas for dealing with the health issues in the vascular system, which include many of the top killers worldwide.

New York, NY, USA Bingmei M. Fu
East Lansing, MI, USA Neil T. Wright

Contents

The Role of Endothelial Surface Glycocalyx in Mechanosensing and Transduction

Ye Zeng, X. Frank Zhang, Bingmei M. Fu, and John M. Tarbell

Abstract

The endothelial cells (ECs) forming the inner wall of every blood vessel are constantly exposed to the mechanical forces generated by blood flow. The EC responses to these hemodynamic forces play a critical role in the homeostasis of the circulatory system. A variety of mechanosensors and transducers, locating on the EC surface, intra- and trans-EC membrane, and within the EC cytoskeleton, have thus been identified to ensure proper functions of ECs. Among them, the most recent candidate is the endothelial surface glycocalyx (ESG), which is a matrix-like thin layer covering the luminal surface of the EC. It consists of various proteoglycans, glycosaminoglycans, and plasma proteins and is close to other prominent EC mechanosensors and transducers. This chapter summarizes the ESG composition, thickness, and structure observed by different labeling and visualization techniques and in different types of vessels. It also presents the literature in determining the ESG mechanical properties by atomic force microscopy and optical tweezers. The molecular mechanisms by which the ESG plays the role in EC mechanosensing and transduction are described as well as the ESG remodeling by shear stress, the actin cytoskeleton, the membrane rafts, the angiogenic factors, and the sphingosine-1-phosphate.

Y. Zeng (✉)
Institute of Biomedical Engineering, West China School of Basic Medical Sciences and Forensic Medicine, Sichuan University, Chengdu, China
e-mail: ye@scu.edu.cn

X. F. Zhang
Department of Mechanical Engineering and Mechanics, Lehigh University, Bethlehem, PA, USA

B. M. Fu · J. M. Tarbell
Department of Biomedical Engineering, The City College of the City University of New York, New York, NY, USA

1 Introduction

The inner wall of every blood vessel in our body is formed by endothelial cells (ECs). Besides biochemical stimuli, blood flow-induced (hemodynamic) mechanical stimuli modulate EC morphology and function by activating mechanosensors, signaling pathways, and gene and protein expressions (Mammoto et al. 2012). EC responses to the hemodynamic forces (mechanosensing and transduction) are critical to maintaining normal vascular functions (Davies et al. 1984; Chien 2007). Failure in mechanosensing and transduction contributes to

B. M. Fu, N. T. Wright (eds.), *Molecular, Cellular, and Tissue Engineering of the Vascular System*, Advances in Experimental Medicine and Biology 1097,
https://doi.org/10.1007/978-3-319-96445-4_1

serious vascular diseases including hypertension, atherosclerosis, aneurysms, stroke, thrombosis, and cancer, to name a few (Ingber 2003; Cai et al. 2012; Fu and Tarbell 2013; Tarbell and Cancel 2016).

The hemodynamic forces that ECs experience include pressure, shear, and circumferential stretch. The force (per unit surface area) perpendicular to the EC (the vessel wall) is the pressure due to the hydrodynamic force generated by the heart. The human circulatory system is ~100,000 miles long, and the magnitude of blood pressure is not uniform in all the blood vessels in the human body. The blood pressure ranges from almost zero to ~120 mmHg for a healthy adult human under resting conditions (Fung 1997). Another type of force (per unit surface area) which is tangential to the EC surface is called shear or shear stress. The shear is due to the friction between the circulating blood and the vessel wall and ranges 10–40 dyn/cm^2 for arterial ECs and 1–6 dyn/cm^2 for venous ECs (Yamamoto and Ando 2011). The third force that acts along the circumference of the vessel wall is named circumferential stretch (or wall tension), also due to the blood pressure. Like the pressure and shear, the stretch varies in different types of vessels and under resting and exercising conditions. These hemodynamic forces vary spatially in different organs (10^{-1}–1 m length scale) and tissues (10^{-2}–10^{-1} m) due to vascular sizes and patterns (e.g., branches and turns), and temporally due to the pulsatile and oscillatory nature of the blood flow in large vessels. Even at the cellular level (10^{-3} m), there is a spatial distribution of these forces (Muller et al. 2004). To sense and transmit the constantly varying hemodynamic forces from the EC surface to its cytoplasm and further into the nucleus, a variety of mechanosensors and transducers (with size in the range from 10^{-9} to 10^{-4} m) are required. So far, at least ten candidates have been identified as mechanosensors and transducers, including cell adhesion proteins (e.g., VE-cadherin, PECAM-1) (Schwartz and DeSimone 2008; Stevens et al. 2008), ion channels (Gojova and Barakat 2005; Gautam et al. 2006), tyrosine kinase receptors (e.g., vascular endothelial growth factor receptor 2) (Schwartz and DeSimone 2008), G-protein-coupled receptors and G-proteins (Yamamoto and Ando 2011), caveolae (Tabouillot et al. 2011), primary cilia (Egorova et al. 2012), actin filaments (Matsui et al. 2011), nesprins (Morgan et al. 2011), integrins (Wang et al. 2009), and endothelial surface glycocalyx (ESG) (Tarbell and Pahakis 2006; Weinbaum et al. 2007; Tarbell and Ebong 2008; Fu and Tarbell 2013).

Endothelial cells are covered by a matrix-like layer called the endothelial surface glycocalyx (ESG) in the present chapter. More generally it may be referred to as the endothelial surface layer (ESL) to emphasize the complexity of the layer and its many components as in F. E. Curry's Chap. 2. Or, for simplicity, it is perhaps most often called the "glycocalyx" to emphasize that proteoglycans, glycoproteins, and glycosaminoglycans are the central components of the surface layer. Due to its unique location, composition, and structure, in addition to serving as a selective permeability, anti-inflammatory, and anti-adhesive barrier at the luminal side of the endothelium, the ESG plays a critical role in EC mechanosensing and transduction to regulate circulation functions (Fig. 1) (Reitsma et al. 2007; Tarbell and Ebong 2008; Curry and Adamson 2012). Because of its proteoglycan and glycosaminoglycan composition, the ESG may cover the entire surface of the EC as shown in Fig. 1 and thus can interact with other EC sensors and transducers to play a role in sensing and transmitting hemodynamic forces.

This chapter only summarizes the literature for the role of ESG as a mechanosensor and transducer. Other roles are presented in Chaps. 2 and 3. The composition, structure, and organization of the ESG are first introduced in the chapter, followed by its mechanical properties. Then the mechanism by which the ESG plays its role in mechanosensing/transduction is elucidated. Finally, the remodeling of ESG by shear stress, the actin cytoskeleton, the membrane rafts, the angiogenic factors, and the S1P is described.

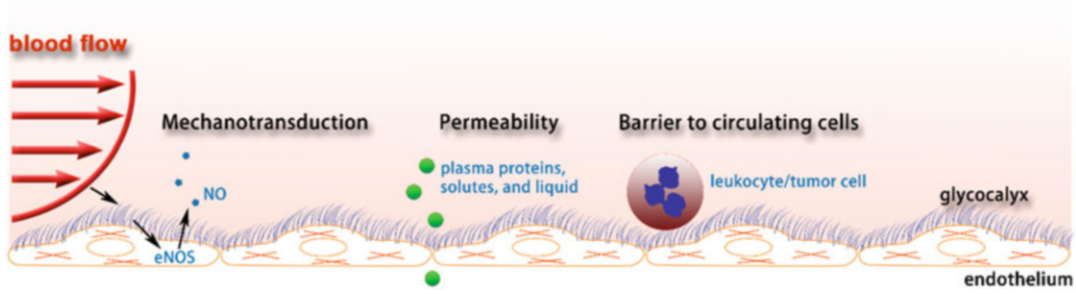

Fig. 1 Roles of endothelial surface glycocalyx (ESG) in regulating circulation functions. The ESG plays at least three roles in maintaining the normal functions of the vascular system, being a mechanosensor and transducer, a molecular sieve, and a barrier between circulating cells such as leukocytes and tumor cells and endothelial cells forming the inner wall of blood vessels

2 Composition, Organization, and Structure of ESG

2.1 Molecular Composition

The roles of mechanosensing and transduction of ESG are based on its molecular composition and organization, which are cartooned in Fig. 2 (Tarbell and Pahakis 2006; Zeng 2017). The components of the ESG have been investigated in depth (Zeng et al. 2012; Tarbell and Cancel 2016). The ESG is mainly composed of glycoproteins bearing short acidic oligosaccharides and terminal sialic acids (SA) and proteoglycans (PG) like heparan sulfate PGs (HSPG) including syndecan and glypican core proteins with long glycosaminoglycan (GAG) side chains. The negatively charged GAGs bind proteins, growth factors, cations, and other plasma components. The predominant GAGs in ECs are heparan sulfate (HS), chondroitin sulfate (CS), and hyaluronic acid (HA). Of the three, the most abundant is HS, accounting for 50–90% of the total GAGs, the rest being comprised of CS and HA (Sarrazin et al. 2011). HS and CS are covalently bound to PGs, whereas HA does not bind to a PG core protein. HA is a non-sulfated GAG, which binds with its surface receptors CD44 and receptor for HA-mediated motility (RHAMM).

The HSPG syndecan family has four members: syndecan-1, syndecan-2, syndecan-3, and syndecan-4. Syndecan-1 contains five potential GAG attachment sites, three near its NH_2-terminal ectodomain and two adjacent to the transmembrane domain near its COOH terminus. CS is only found near the COOH terminus of syndecan-1 (Tarbell and Pahakis 2006). Syndecan-3 contains eight potential GAG attachment sites, five near its NH_2-terminal ectodomain and three adjacent to the transmembrane domain near its COOH terminus. Both syndecan-2 and syndecan-4 contain three potential GAG attachment sites near their NH_2-terminal ectodomain (Bernfield et al. 1999; Lopes et al. 2006). Syndecan-4 can also contain CS and is often located on the basal side of the cell (Deepa et al. 2004). In the HSPG glypican family, only glypican-1 is expressed in ECs. Glypican-1 is a membrane glycosylphosphatidylinositol (GPI)-anchored protein, which only binds with HS. GPI-anchored protein is localized in both lipid rafts and caveolae (Lisanti et al. 1994; Schnitzer et al. 1995a). The formation and function of caveolae is dependent on phosphorylation of caveolin-1 which is induced in a HA-dependent manner (Long et al. 2012). Some fractions of HA bound to CD44 are internalized into caveolae (McGuire et al. 1987; Tarbell and Pahakis 2006). The internalized caveolae might fuse with caveosomes, thus playing an important role in transcytosis of its contents such as albumin (Schubert et al. 2001; Nichols 2003). Sphingosine-1-phosphate (S1P) protects glycocalyx that is required for

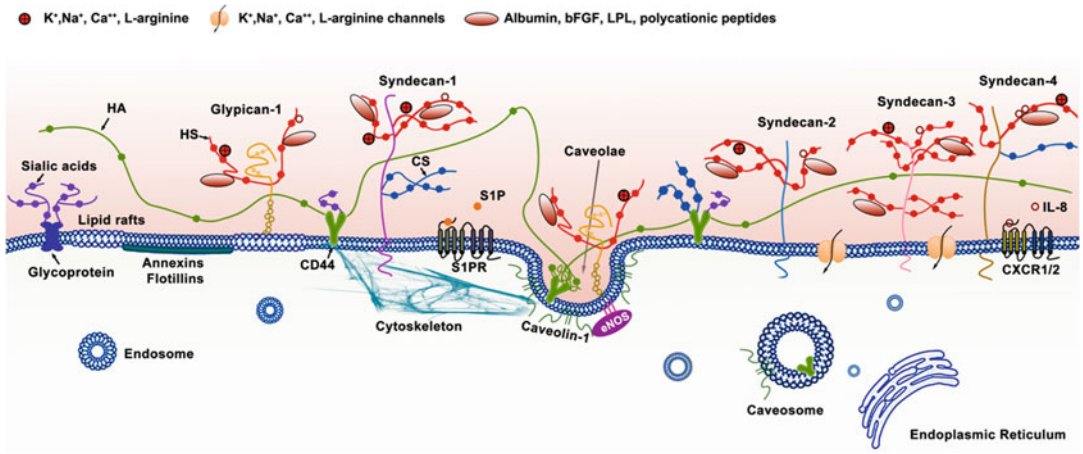

Fig. 2 Structural components of the endothelial glycocalyx. The ESG is mainly located at the luminal side of vascular ECs although syndecan-4 is dominantly basal. The apical GAGs and associated proteins and ions are directly in contact with the bloodstream, and they transfer flow forces to the core proteins that transmit them to the cell. In addition to bound plasma components, the ESG is mainly composed of glycoproteins bearing acidic oligosaccharides and terminal sialic acids (SA); proteoglycans (PG), such as heparan sulfate proteoglycans (HSPGs, syndecan family and glypican-1); and GAG side chains. The predominant GAGs in ECs are heparan sulfate (HS), chondroitin sulfate (CS), and hyaluronic acid (hyaluronan, HA). HS and CS are attached to PGs. HA binds with receptor CD44. Syndecans (including syndecan-1, syndecan-2, syndecan-3, and syndecan-4) are single transmembrane domain proteins. Glypican-1 is a membrane glycosylphosphatidylinositol (GPI)-anchored protein, which is localized in lipid rafts, as well as caveolae. Lipid rafts are characterized by high translational mobility. Integrity of the actin cytoskeleton is essential for the immobility of caveolae. Syndecan-1 and CD44 interact with the cytoskeleton. Annexins and flotillins might be involved in the formation and function of caveolae. Some fraction of HA bound to CD44 are internalized into caveolae. The phosphorylation of caveolin-1, a protein responsible for maintaining the shape of caveolae, is induced in a HA-dependent manner, which might be involved in CD44-caveolae-mediated endocytosis. It has been assumed that internalized caveolae fuse with caveosomes. Caveosomes play an important role in transcytosis of its contents such as albumin to other subcellular (non-lysosomal) compartments including the endoplasmic reticulum in ECs. Sphingosine-1-phosphate (S1P) protects the shedding of glycocalyx and induces the synthesis of glycocalyx that is required for mechanotransduction and cytokine response (i.e., IL-8/CXCR1/2-induced EC migration) (Revised from Tarbell and Pahakis (2006); Zeng (2017))

mechanotransduction and cytokine response (i.e., IL-8/CXCR1-/CXCR2-induced EC migration (Tarbell and Pahakis 2006; Weinbaum et al. 2007; Tarbell and Ebong 2008; Fu and Tarbell 2013; Zeng et al. 2013; Zeng et al. 2014; Zeng and Tarbell 2014; Zeng et al. 2015; Yan et al. 2016).

In resting conditions, syndecans and glypican-1 mRNAs in human umbilical vein endothelial cells (HUVECs) are expressed in the order: syndecan-1 > syndecan-4 > syndecan-3 > syndecan-2 > glypican-1 (Liu et al. 2016). The ESG is modified under several conditions including disturbed flow exposure in large vessels (Brands et al. 2007), protease degradation (Huxley and Williams 2000; Brands et al. 2007; Lipowsky 2012), and removal of plasma components, particularly albumin (Michel et al. 1985).

2.2 Organization

It is widely believed that the negatively charged GAGs in the ESG capture circulating plasma proteins and cations and form an interconnected gel-like structure in an aqueous environment (Ohlson et al. 2001; Sorensson et al. 2001; Weinbaum et al. 2007) and that the ESG would collapse if a GAG component was significantly reduced. However, a recent study by Zeng et al. (2012) observed that specific enzymatic removal of HS or HA did not result in cleavage or collapse of

any of the remaining components. Simultaneous removal of CS and HA by chondroitinase did not affect HS. Their results suggest that all GAGs and adsorbed proteins are well intermixed within the structure of the ESG but the GAG components do not interact with one another.

2.3 Thickness and Structure

In addition to its biochemical composition, the thickness and ultrastructure of the ESG determine its function as a mechanosensor and transducer. The first visualization of the ESG by electron microscopy (EM) used the cationic dye ruthenium red that binds to acidic mucopolysaccharides and generates electron density in the presence of osmium tetroxide (Luft 1966). Subsequent studies (Baldwin and Winlove 1984; Sims and Horne 1993) used gold colloids and immunoperoxidase labeling. Adamson and Clough (1992) then demonstrated using a large charged marker protein (unable to penetrate the ESG), cationized ferritin (molecular weight ~450 kDa), that in the absence of plasma proteins, the ESG would collapse, presumably due to elimination of intramolecular interactions with plasma proteins, and that its undisturbed thickness was several times greater than the 20 nm observed with ruthenium red (Luft 1966). All of these methods may suffer from dehydration artifacts associated with aqueous fixatives that likely dissolve all but the protein cores of proteoglycans and collapse the inherently hydrated structures. A method developed to preserve water-soluble structures using fluorocarbons as nonaqueous carriers of osmium tetroxide was applied to microvessels to obviate some of these limitations by Sims and Horne (1993). Further elaborations of the fluorocarbon-glutaraldehyde fixation methods by Rostgaard and Qvortrup (1997) revealed a filamentous brush-like surface coating on capillary walls, but a layer thickness of less than 50 nm, suggesting a cleavage of more superficial matrix structures. All of the foregoing EM studies revealed an ESG with a thickness less than 100 nm. Recently, van den Berg et al. (2003) used a new approach to stabilize the anionic carbohydrate structure on the ESG by Alcian Blue 8GX (Fig. 3). They found that the ESG thickness was 0.2–0.5 μm on rat left ventricular myocardial capillaries.

To overcome the artifact by EM, the amount of ESG was estimated based on the biophysical principles from in vivo observations (Klitzman and Duling 1979). A direct in vivo measurement of the ESG thickness with the dye-exclusion technique was developed by Vink and Duling (1996). Using a 70 kD FITC-dextran plasma tracer, which they showed was sterically excluded by the ESG, they were able to provide the first estimate of the in vivo thickness of the ESG in capillaries of hamster cremaster muscle to be ~0.4–0.5 μm. Most recently, the ESG thickness was also estimated as ~0.5 μm in rat mesenteric postcapillary venules by FITC-dextran labeling with intravital microscopy (Long et al. 2004). This estimate of the in vivo thickness of the ESG is four to five times greater than previous estimates derived from EM studies. This discrepancy was a catalyst for much of the work that has followed on the estimation of ESG thickness and its function as a barrier in cellular interactions as well as a mechanosensor and transducer of ECs. Using high-resolution, near-wall, intravital fluorescent microparticle image velocimetry (μ-PIV) to examine the velocity profile near the vessel wall in postcapillary venules of the mouse cremaster muscle, Long et al. (2004) and Smith et al. (2003) produced estimates of glycocalyx thickness of order 0.5 μm.

The poor spatial resolution of an intravital optical microscope limits the accurate measurement of the ESG thickness (Pries et al. 2000). New imaging methods have thus been developed by employing laser scanning confocal microscopy and multi-photon microscopy, and fluorescently tagged antibodies to HS or HA binding protein, or wheat germ agglutinin to label major components of the ESG. Application of these new methods has revealed a much thicker ESG in large blood vessels: 4.3–4.5 μm in the mouse common carotid artery (van den Berg et al. 2009), 2.2 μm in the mouse internal carotid artery (Reitsma et al. 2011), and 2.5 μm in the external carotid

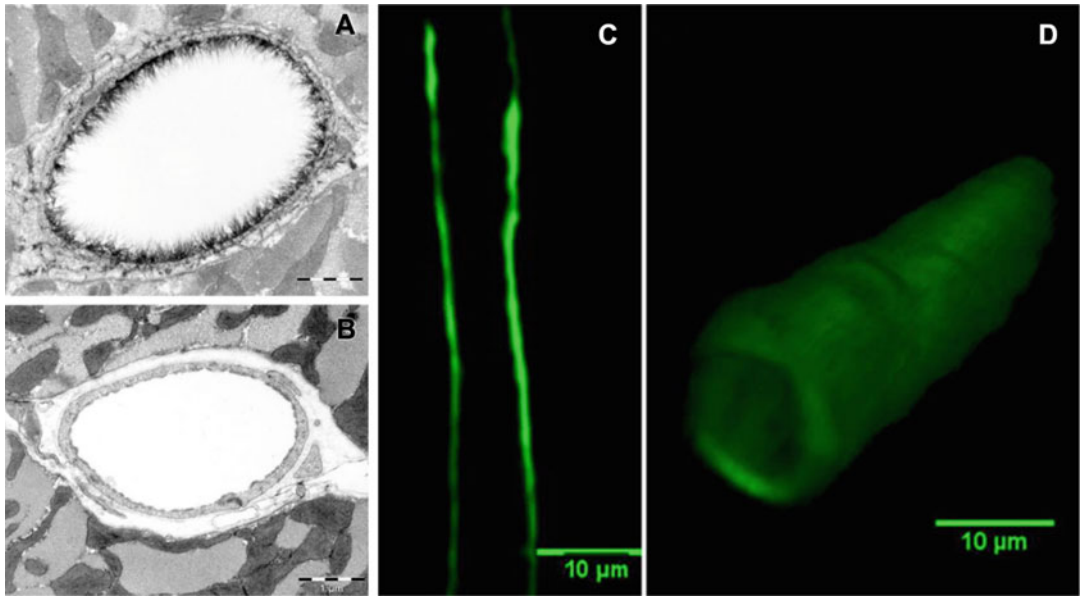

Fig. 3 The ESG at the microvessel wall observed by different visualization techniques. Left, electron microscopic view of an Alcian Blue 8GX-stained ESG on rat left ventricular myocardial capillary (**a**) after enzyme treatment to remove the ESsG (**b**). Scale bar is 1 μm. From Van den Berg et al. (2003). Right, confocal microscopic view of anti-HS labeled ESG on rat mesenteric capillaries. Midplane view (**c**) and 3D view (**d**). From Yen et al. (2012)

artery (Megens et al. 2007). Ebong et al. (2011) presented the first cryo-EM images of in vitro ESG that avoided the dehydration artifacts of conventional EM and observed structures greater than 5 μm in thickness (up to ~11 μm). Most recently, using high-sensitivity and high-resolution confocal microscopy and in situ/in vivo single microvessel and ex vivo aorta immunostaining, Yen et al. (2012) revealed that the thickness of the ESG on rat mesenteric and mouse cremaster capillaries and postcapillary venules is 1–1.5 μm. Surprisingly, there was no detectable ESG in arterioles by using fluorescence labeled anti-HS. The ESG thickness is 2–2.5 μm on rat and mouse aorta. They also observed that the ESG is continuously and evenly distributed on the aorta wall but not on the microvessel wall if looking at a vessel segment of length ~100 μm. By comparing the distance between the plasma membrane labeling and the labeling of ESG (SA residues) by wheat germ agglutinin (WGA) in a single microvessel in vivo, Betteridge et al. (2017) found that the ESG thickness is 0.17–3.02 μm in the same type of microvessels as in Yen et al., (2012), depending on the labeling and analyzing methods. However, the thickness of ESG at the same portion of the vessel is only ~0.08 μm observed by the EM through Alcian Blue labeling.

The ultrastructural organization of the ESG and its relation to the cytoskeleton components (e.g., F-actin) of ECs was first investigated by Squire (2001). Using computed autocorrelation functions and Fourier transforms of EM images of frog mesenteric microvessels, they identified a quasi-periodic substructure in the ESG, which is a 3D fibrous meshwork with characteristic spacing ~20 nm. The fiber diameter was observed as 10–12 nm. They also showed that the fibrous elements may occur in clusters with a common intercluster spacing of ~100 nm and may be linked to the underlying actin cortical cytoskeleton. The recent study by Arkill et al. (2011) observed similar ESG structures in mammalian microvessels of choroid, renal tubules, glomerulus, and psoas muscle and was confirmed by a 3D reconstruction using electron tomography by employing a tannic acid staining method

and a novel staining technique of lanthanum dysprosium glycosaminoglycan adhesion (the LaDy GAGa method) (Arkill et al. 2012). The thickness of the ESG observed by their EM method is ~100 nm, similar to what was previously found on frog mesenteric microvessels (Adamson and Clough 1992). The approximately 100 nm thick structure may form an inner core of the ESG which determines the filtration and molecular sieve function of the microvessel wall to water and solutes while a micron scale outer structure may generate a buffer region for the lubrication of RBC movement and a barrier for WBC adhesion to the ECs forming the vessel wall. But how this structure plays a role in mechanosensing and transduction remains to be elucidated. The two-layer model is discussed further in reference to permeability properties in the chapter by Curry.

The recent development of ultra-resolution stochastic optical reconstruction microscopy (STORM) has made it possible to visualize the ESG structure at high resolution (Zullo et al. 2016; Song et al. 2017). STORM employs organic dyes and fluorescent proteins as photo-switchable emitters to trade temporal resolution for a super spatial resolution (20 nm lateral and 50 nm axial at present due to the size of antibodies used to identify the ESG components), which is an order of magnitude greater than conventional confocal microscopy (Rust et al. 2006). Future studies by using STORM along with much smaller peptides instead of antibodies to identify the ESG components should elucidate the ultrastructure and molecular composition of ESG in fresh cell and tissue samples. Another method of combining lanthanum dysprosium glycosaminoglycan adhesion staining and electron tomography (Arkill et al. 2012) can also reveal the ultrastructure at high resolution.

3 Mechanical Properties of Glycocalyx

To sense and transmit the blood flow-induced forces from the ESG surface to the EC cell body and nucleus, it is necessary for the ESG fibers (core proteins and attached GAGs) to have a structural integrity, which is characterized by the flexural rigidity, EI. Applying a linear elasto-hydrodynamic model, Weinbaum et al. (2003) predicted that EI of the ESG fibers is 700 pN nm^2 by matching the time-dependent restoration of the ESG after being crushed by the passage of a WBC in a tightly fitting capillary (Vink and Duling 1996). Later, Han et al. (2016) developed a more sophisticated nonlinear elastohydrodynamic model that uses large deformation theory for elastica and a modified Brinkman equation to describe the local relative motion of the fibers and the fluid. Their prediction for the EI of the ESG fibers is 490 pN nm^2, comparable to the result predicted by the earlier linear model (Weinbaum et al. 2003). Nijenhuis et al. (2009) used optically trapped submicron probe particles to measure the viscoelastic properties of an in vitro ESG model, which consists of a 2.5 mg/mL bulk solution of hyaluronan (HA) and other components of the ESG, including CS, HS, aggrecan, albumin, and plasma. They found that CS and aggrecan, which directly interact with HA, modify the viscoelastic properties of the HA solution, while HS, plasma, and albumin have no effects.

Applying atomic force microscopy (AFM) microindentation method, the elastic modulus of the ESG on bovine lung microvascular EC (BLMVEC) monolayer was measured as ~0.3 kPa after enzyme treatment for HS and HA (O'Callaghan et al. 2011). By using an AFM nanoindentation method, a more recent study by Bai and Wang (2012) determined Young's modulus of the ESG on HUVEC monolayer to be 0.39 kPa. Due to its loose structural network and high water content, the ESG is approximately one order of magnitude softer than the plasma membrane. Oberleithner et al. (2011) were able to quantify the stiffness and thickness of ESG from AFM force-indentation curves. This method is shown in Fig. 4. Light microscopy was used to ensure that the AFM tip was located neither at the nuclear, nor at the junctional region of cultured ECs (Fig. 4a). In some experiments, the cells were stained with wheat germ agglutinin-FITC to simultaneously monitor the intactness of ESG (Fig. 4b, insets). During the indentation scan, the AFM tip travels vertically

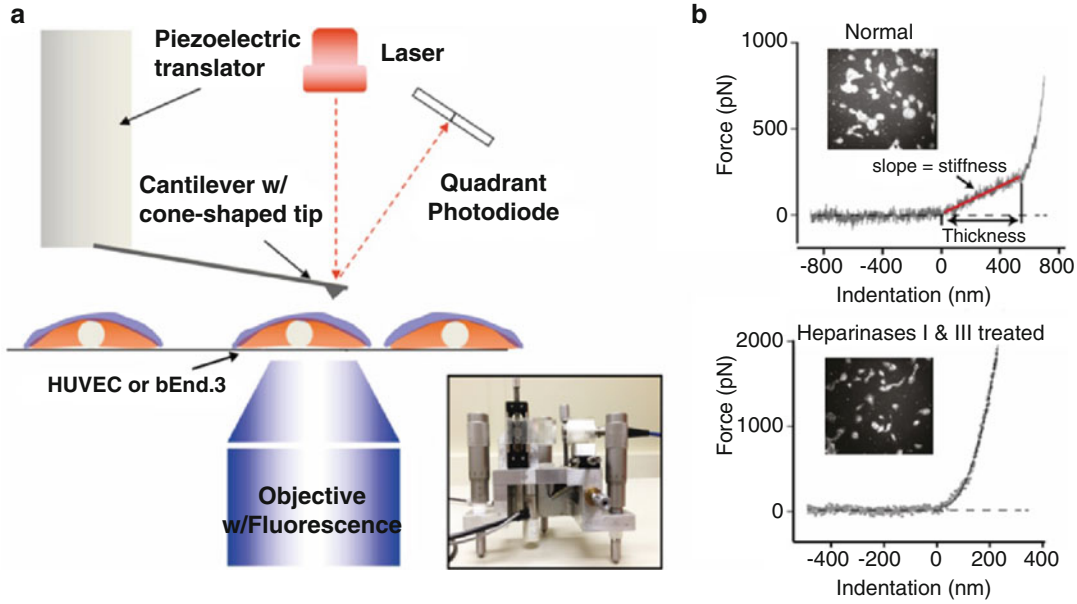

Fig. 4 AFM nanoindentation. (**a**) A schematic diagram of the AFM assay. Insert: a picture of the AFM head used for nanoindentation. The blue layer on cell surface indicates the ESG. (**b**) Quantification of thickness and stiffness of ESG by AFM nanoindentation. Cited from Song et al. (2017)

toward the HUVEC surface. Upon indentation of the ESG, the AFM cantilever, serving as a soft spring, is deflected (boxed region in Fig. 4b upper panel). The cantilever deflection is measured and plotted as a function of sample position along the *z*-axis. The resulting curve is transformed into a force-versus-indentation curve using the cantilever's spring constant and the light lever sensitivity. The slope of a force-indentation curve directly reflects the stiffness (expressed in pN/nm), which is necessary to indent the ESG for a certain distance. The first slope indicates the stiffness (in this trace 0.30 pN/nm) of the very first layer, which is the ESG. The second nonlinear region indicates the stiffness of the plasma membrane. The distance between the starting point of ESG indentation and the starting point of the second slope (projected to the *x*-axis) corresponds to the thickness of the EG (in this trace ~550 nm). In average, ESG on HUVECs has an averaged thickness of 651 ± 54 nm and stiffness of 0.25 ± 0.07 pN/nm. Treatment of HUVECs with heparinases I and III eliminated the linear spring region of the force-indentation curve, indicating that the EG was degraded by enzymatic digestion. Using this method, Oberleithner et al. (2011) further showed that sodium overload led to stiffened and thinner (i.e., collapsed) ESG, whereas treatment of ECs with thrombin, lipopolysaccharides, or tumor necrosis factor-α reduced both EG stiffness and thickness (Fels et al. 2014). Instead of simply treating the ESG force-indentation curve as a linear slope, a two-layer Hertzian model has been used by Marsh and Waugh (2013) to fit the nanoindentation curves, yielding ESG elastic modulus of 0.7 ± 0.5 kPa and thickness of 380 ± 50 nm.

4 Mechanotransduction and ESG

An important function of the ESG is to serve as a mechanosensor and transducer (Tarbell and Pahakis 2006; Weinbaum et al. 2007; Tarbell and Ebong 2008; Fu and Tarbell 2013; Haeren et al. 2016; Tarbell and Cancel 2016). It is well known that a dysfunctional endothelium is an early manifestation of atherosclerosis (AS) (Yurdagul Jr.

et al. 2016). Vascular endothelial injury in AS-susceptible locations is a prerequisite for AS formation (McAlpine and Swirski 2016; Sorci-Thomas and Thomas 2016; Taleb 2016).

In AS-susceptible locations such as branches, bifurcation, and curvatures (e.g., the aortic arch) of the arterial tree, the blood stream undergoes tremendous interference, and the flow departs from pulsatile, unidirectional shear stress to create flow separation zones that include flow reversal, oscillatory and multi-directional shear stress, and sometimes turbulence (chaotic flow) (Davies 2009; Zhou et al. 2014; Dabagh et al. 2017). In contrast, flow in adjacent undisturbed flow regions of the arteries is pulsatile and has unidirectional flow direction with minimal reversal. It has been speculated that low shear stress induces the initial lesion, and high shear stress promotes the formation of calcified vulnerable plaques (Wang et al. 2016; Eshtehardi et al. 2017).

The ESG plays an important role in EC mechanotransduction of shear stress. Weinbaum et al. (2003) pointed out that the existence of the ESG could reduce the fluid shear stress on the vascular EC surface to a negligible level by theoretical analysis, while Secomb et al. (2001) described the transfer of fluid mechanical shear stress at the interface between the fluid and the outer regions of the ESG to solid mechanical stress within the matrix. Thi et al. (2004) further showed that the ESG is required for the EC cytoskeleton to respond to shear stress.

Florian et al. (2003) showed that enzymatic removal of HS from the surface of BAECs in vitro completely blocked shear-induced NO production in both steady flow (15 dyn/cm^2) and reversing oscillatory flow (10 ± 15 dyn/cm^2) out to 3 h exposure including both the early phase (seconds to minutes after a step increase in shear) that is calcium and G-protein dependent as well as the later phase (minutes to hours) that is independent of calcium and G-protein (Kuchan et al. 1994). Yen et al. (2015) demonstrated that degradation of HS in the rat mesentery greatly inhibited NO production in response to an increase in flow. Pahakis et al. (2007) showed that shear-induced NO production was blocked by enzymes removing HS and HA, but not CS and that these treatments had no effect on the shear-induced production of the important vasodilator and antiplatelet agent, prostacyclin (PGI_2). Because the proteoglycan core protein glypican-1 only binds HS and not CS and the dominant apical syndecan (syndecan-1) binds both HS and CS, it was hypothesized that glypican-1 is the core protein that transmits the fluid shear force sensed by the GAG (HS) to the cell surface where it is ultimately transduced via the phosphorylation of eNOS into NO. This hypothesis was tested by Ebong et al. (2014) who showed that knockdown of glypican-1 using shRNA completely blocked shear-induced phosphorylation of eNOS, whereas knockdown of syndecan-1 had no effect. Because knockdown of genes by shRNA can have off-target effects, the hypothesis was further tested using atomic force microscopy (AFM) with cantilevers coated with specific antibodies to HS, glypican-1, and syndecan-1 (Bartosch et al. 2017). Force applied to HS or glypican-1 resulted in NO production, whereas force applied to syndecan-1 did not. These experiments were carried out at 10 and 30 min and did not specifically interrogate the early G-protein-dependent phase of activation.

Zeng and Liu (2016) found that shear stress has a dual role in eNOS activation: 4 dyn/cm^2 shear stress inhibited the activation of eNOS, and 15 dyn/cm^2 shear stress induced it. Removal of glypican-1 by phosphatidylinositol phospholipase C (PI-PLC) significantly suppressed the 15 dyn/cm^2 shear stress-induced eNOS activity and further reduced the 4 dyn/cm^2-inhibited eNOS activity (Zeng and Liu 2016). Therefore, eNOS activation depends on shear stress magnitudes and is mediated by glypican-1.

To follow-up on the observation that GAG removal by enzymes did not block shear-induced PGI_2 production (Pahakis et al. 2007), Russell-Puleri et al. (2017) investigated primary cilia, syndecan-4, and platelet endothelial cell adhesion molecule 1 (PECAM-1), as potential mechanosensors for PGI_2 production. Primary cilia are localized to the apical surface of EC and syndecan-4 to the basal surface and in confluent ECs PECAM-1 localizes at intercellular junctions where it regulates homophilic binding between cells. Separate knockdown of the

three putative mechanosensors in cultured cells revealed that only PECAM-1 deletion blocked shear-induced PGI_2 production and upregulation of the enzyme cyclooxygenase 2 (COX-2) by a mechanism involving inside-out activation $\alpha_5\beta_1$ integrin. The role of PECAM-1 in shear-induced PGI_2 was further confirmed in a PECAM-1 knockout mouse model (Russell-Puleri et al. 2017). Conway et al. (2013) using a fluorescence resonance energy transfer (FRET) tension sensor, showed that shear stress increased tension across PECAM-1 at intercellular junctions. Weber et al. (2017) applied tension to the extracellular domain of PECAM-1 using AFM and observed upregulation of COX-2, the precursor to PGI_2 production.

In related studies, it has been shown that PECAM-1 is also an upstream mediator of shear stress-induced NO production. Fleming et al. (2005) and Wang et al. (2015) observed that shear stress-induced tyrosine phosphorylation of PECAM-1 as well as the serine phosphorylation of Akt and eNOS was abolished by pretreatment of cells with a tyrosine kinase inhibitor. A comparable attenuation of Akt and eNOS phosphorylation and NO production was also observed in endothelial cells generated from PECAM-1-deficient mice. Xu et al. (2016) found that flow-mediated eNOS phosphorylation in vivo induced by voluntary wheel running was reduced in PECAM-1 knockout mice. However, when the extracellular domain of PECAM-1 was put under tension by AFM with the same specific antibody that led to COX-2 upregulation, there was no effect on NO production (Bartosch et al. 2017).

How can we reconcile the observations that the proteoglycan core protein glypican-1 mediates shear-induced eNOS phosphorylation and NO production (Ebong et al. 2014; Bartosch et al. 2017) with similar findings for PECAM-1 (Fleming et al. 2005; Xu et al. 2016)? Our working hypothesis is that the upstream shear stress sensor is glypican-1 that activates intracellular signaling pathways leading to tyrosine phosphorylation of PECAM-1 and downstream serine phosphorylation of eNOS and NO production. This most likely corresponds to the later phase of NO production since all of the supporting experiments were conducted in a time frame of minutes to hours.

The glycocalyx might also play an important role in early-phase mechanotransduction in response to a step change in shear stress through the interaction between the G-protein Gαq/11 and PECAM-1 (dela Paz et al. 2014). It has been shown that PECAM-1 and Gαq/11 form a mechanosensitive complex that contains an endogenous HSPG with HS chains that is critical for junctional complex assembly and regulation of the flow response. In experiments that used heparinase to cleave HS, such as Florian et al. (2003), Pahakis et al. (2007), and others, the PECAM-1/Gαq/11 complex bound by HS would have been disrupted thus altering the early-phase induction of NO production. This would be consistent with the observation by Florian et al. (2003) that heparinase treatment blocked both the early and later phase response of NO production to a step change in shear stress.

Synthesizing the above discussion of mechanisms for shear-PECAM-1-COX-2-PGI_2, the early phase shear- Gαq/11/PECAM-1-NO, and the sustained phase shear-Glypican-1-PECAM-1-NO, we arrive at the overall hypothesis summarized in Fig. 5. It should be noted that the cartoons of Figs. 5, 6, and 8 emphasize the central components of the mechanisms. They do not, for example, include the detailed components of the surface layer that may be involved in transmitting fluid shear stress to the proteoglycan core proteins glypican-1 and syndecan-1. These were shown in greater detail in Fig. 2 and discussed earlier in this section.

5 Remodeling of ESG

5.1 Shear Stress and ESG

Several studies have detected a substantial glycocalyx on cultured rat fat pad EC (RFPECs) (Thi et al. 2004; Ebong et al. 2011; Zeng et al. 2012). In a recent study using fluorescence confocal microscopy (Zeng et al. 2012), it was shown that the coverages of HS and CS on RFPECs under

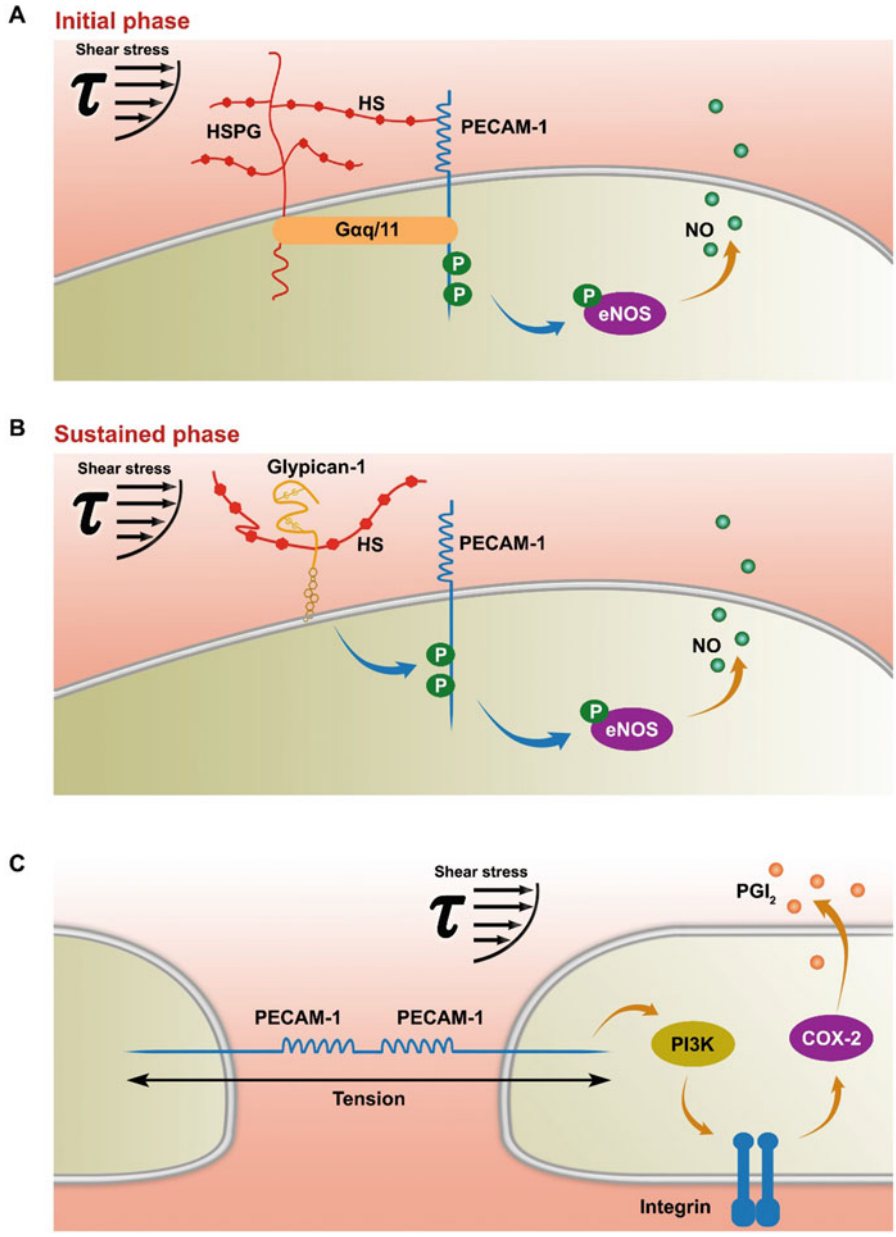

Fig. 5 Proposed mechanism of shear stress-induced NO and PGI_2. (**a**) Gαq/11/PECAM-1 bound by HS is the early phase mechanosensor for NO. (**b**) Glypican-1 is the sustained-phase shear stress sensor that leads to intracellular activation of PECAM-1 and downstream NO production. (**c**) Shear stress-induced tension on PECAM-1 induces PGI_2 production through a PI3K-Integrin-COX-2 signaling pathway

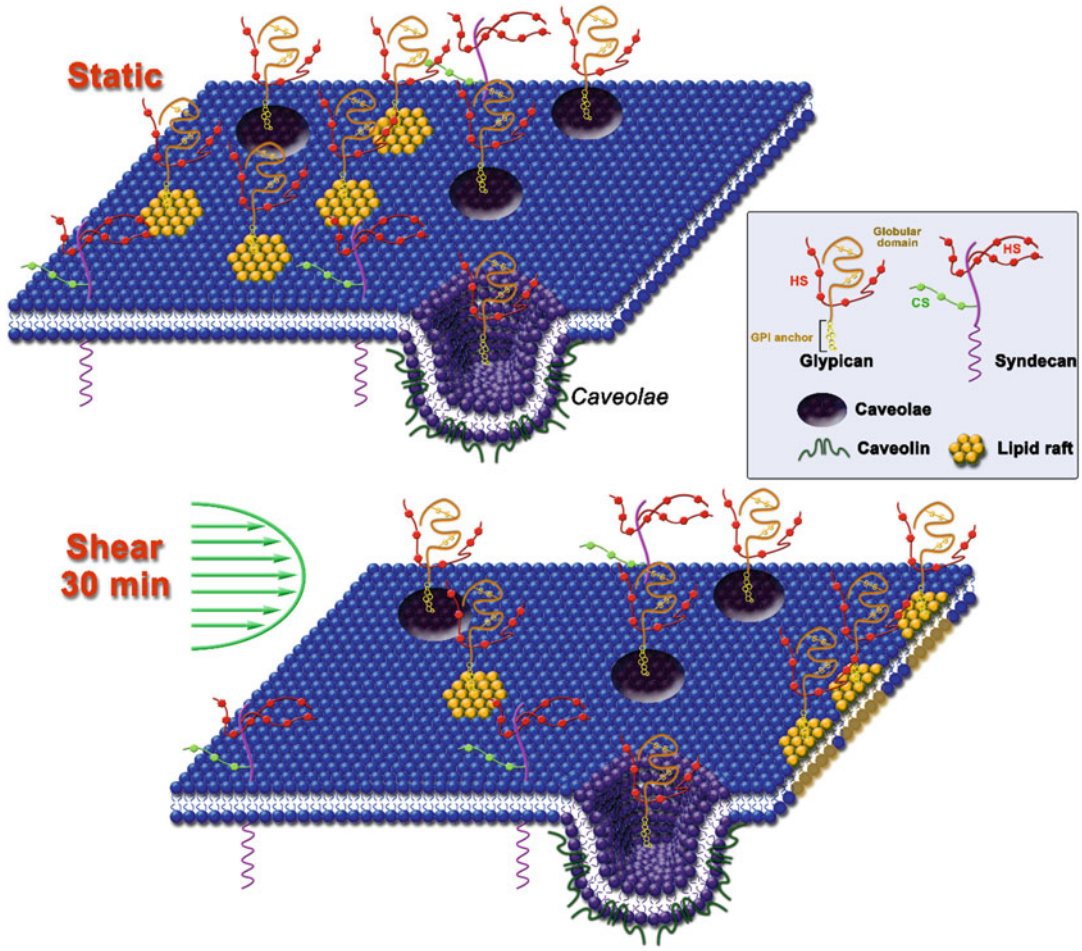

Fig. 6 Early responses of glycocalyx: fluid shear stress induces the clustering of HS via mobility of glypican-1 in lipid rafts. Under static conditions, syndecan-1 is localized outside of caveolae, while GPI-anchored glypican-1 is localized in membrane rafts including both lipid rafts and caveolae. Glypican-1 exclusively carries HS, and syndecan-1 contains CS and HS. After the initial 30 min of exposure to shear stress, lipid rafts with their anchored glypican-1 and associated HS move toward the cell junction. In contrast, the transmembrane syndecan-1 with attached HS and CS, and albumin, seem to be fixed in position, as well as the glypican-1 in caveolae. Cited from Zeng et al. (2013)

static condition are similar, but they cannot infer from this that the relative abundances (masses) are the same or similar. It must be noted that the fluorescent antibody technique can be used to map the location of target antigens, but it cannot be used to compare masses of different molecules because the specific antibody-antigen affinities may differ greatly (Thomas J. Kindt et al. 2007).

Recall that glypican-1 carries HS exclusively, and syndecan-1 carries both CS and HS. Using fluorescence confocal microscopy, it was shown that, in response to 30 min shear stress, glypican-1 was reduced in coverage and appeared to cluster near the cell boundary without expression reduction, but syndecan-1 did not appear to move (Zeng et al. 2013). In addition, by examining MFI data, there was no evidence that HS and CS or glypican-1 and syndecan-1 increased or decreased under shear stress for 30 min. These observations based on fluorescent antibody technique further confirmed that glypican-1, but not syndecan-1, redistributes in response to shear

(Zeng et al. 2013). These results combined with the observation of clustering of HS, but not CS, strongly suggest that glypican-1 carried the HS that moved and aggregated in the cell junction. Notably, glypican-1 is bound directly to the plasma membrane through a GPI anchor and localized to membrane rafts (MRs) (Tarbell and Pahakis 2006).

The MRs consist of dynamic assemblies of cholesterol and sphingolipids, in the exoplasmic leaflet of the bilayer (Lindner and Naim 2009). MRs are classified into two types: protein-based membrane domains (i.e., caveolae) and lipid-based domains (i.e., lipid rafts) (Lindner and Naim 2009; Zeng et al. 2013). Caveolae and lipid rafts exist separately on the cell surface (Schnitzer et al. 1995b); both are greatly enriched in cholesterol and exoplasmic sphingolipids. GPI-anchored proteins are localized in both caveolae and lipid rafts—with nearly half of GPI-anchored proteins localized outside of caveolae on ECs (Lisanti et al. 1994; Schnitzer et al. 1995a). The cholera toxin B subunit (CTx-B), which binds specifically to a component of the plasma membrane—glycosphingolipid, ganglioside GM_1—has been used as a MR marker in many studies (Parton 1994; De Haan and Hirst 2004). GM1 is present over the entire cell surface and enriched in caveolae (Parton 1994). Caveolin-1, which anchors caveolae to the actin cytoskeleton (Navarro et al. 2004), attaches to the cytosolic face of plasma membrane via a hydrophobic hairpin loop and provides a scaffold for caveolae formation (Razani et al. 2002). Caveolin-1 has emerged as a vital plasma membrane mechanosensor (Parton and del Pozo 2013). Meanwhile integrity of the actin cytoskeleton is essential for the immobility of caveolae (Thomsen et al. 2002). In contrast, lipid rafts are held together by specific lipid-lipid interactions (Lingwood and Simons 2010), organized in a liquid-order phase, and characterized by limited acyl chain order but high translational mobility (Lindner and Naim 2009; Simons and Sampaio 2011).

A recent study has demonstrated the changes in distribution of MRs (caveolin-1 and GM_1) after exposing statically cultured RFPECs to shear stress, focusing on the first 30 min after initiation of shear (Zeng et al. 2013). Under shear stress for 30 min, the expression and distribution of caveolin-1 did not change, indicating that caveolae are stabilized sufficiently to resist shear stress during the first 30 min of exposure. In a previous study (Rizzo et al. 2003), it was shown that the caveolae density at the plasma membrane increased sixfold after 10 dyn/cm^2 of shear stress exposure for 6 h—a much longer shear exposure than the 30 min. Although almost all caveolin-1 is localized in caveolae, nearly half of the GPI-anchored proteins reside outside caveolae on ECs (Lisanti et al. 1994; Schnitzer et al. 1995a). A large fraction of glypican-1 was likely associated with caveolae and thus was not mobilized during the 30 min of shear exposure (Zeng et al. 2013), which resulted in the smaller changes in the distribution of glypican-1 compared to HS. Thus, Zeng et al. (2013) concluded that the mobile HS is bound to glypican-1 that is outside the caveolar fraction of membrane rafts. This leads to the conclusion that lipid rafts carry the mobile glypican-1 and HS. The observation of movement of a membrane raft marker—GM_1—has further reinforced this conclusion (Zeng et al. 2013). This mechanism is summarized in Fig. 6.

The dramatic change in HS distribution was confirmed on often studied BAECs (Fig. 7) (Zeng and Tarbell 2014). After 24 h of exposure, BAECs were remodeled into an elongated (fusiform) shape whereas RFPECs retained their cobblestone morphology at 24 h (Zeng and Tarbell 2014). Other EC types as well do not elongate in response to sustained shear stress. For example, during exposure to 40 dyn/cm^2 for 24 h, pig aortic ECs did not align along the flow direction (Arisaka et al. 1995). The BAECs did maintain cobblestone morphology after 30 min of shear exposure. (Zeng and Tarbell 2014).

Similar phenomena occurred on RFPECs and BAECs showing consistent changes in the synthesis and reorganization of HS. The distributions of HS and glypican-1 became nonuniform after 30 min of shear exposure (clustering at the cell boundary) and then returned to a nearly uniform distribution between 30 min and 24 h (Zeng and Tarbell 2014). The distributions of CS

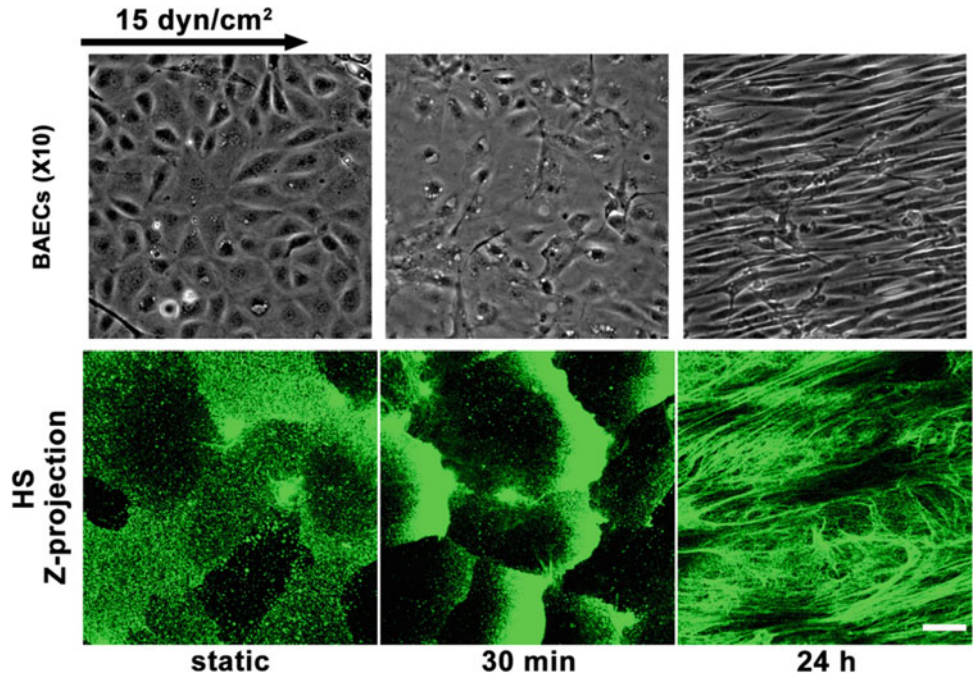

Fig. 7 Validation of the clustering and subsequent restoration of HS under shear stress using bovine aortic endothelial cells. Top: phase contrast micrographs of confluent BAEC monolayer reveal a typical dynamic change in cell morphology from cobblestone (static control) to the elongated (fusiform) and oriented in the direction of flow. Bottom: representative immunofluorescent images of HS under static and shear stress conditions. Figure adapted with permission from (Zeng and Tarbell 2014)

and syndecan-1 were not altered throughout the duration of shear exposure. The in vivo state was examined in Yen et al. (2012) where it was shown that the fully adapted state in the aorta of rats and mice shows a highly uniform coverage of HS that is similar to the 24 h state (Zeng and Tarbell 2014) (Fig. 7). Other glycocalyx components have not yet been examined in vivo.

The adaptation of the glycocalyx to fluid shear stress involves a balance between the synthesis of glycocalyx components including both GAGs and core proteins and their degradation that is modulated by enzymes such as heparanase and metalloproteases (Lipowsky 2011; Curry and Adamson 2012). Zeng and Tarbell (2014) concluded that glycocalyx components were synthesized in RFPECs and BAECs during shear exposure for 24 h, which is consistent with other studies in pig aortic EC (Arisaka et al. 1995) and human EC-RF24 cells (Gouverneur et al. 2006) showing that shear stress induces new synthesis of HS and CS. Recently, Koo et al. (2013) examined the effect of pulsatile flow on glycocalyx formation in cultured HUVECs. They reported that their atheroprotective waveform (high mean shear, no reversal) induced increases in HS and syndecan-1, a decrease in glypican-1, and no alteration of CS after 7 days of exposure. Another study showed that glypican-1 did not change on HUVECs exposed to the atheroprotective waveform for 3 days (Koo et al. 2011).

Notably, the mechanisms underlying the shear stress-induced increase in GAG synthesis are still not known. GAG synthesis induced by shear stress was concomitant with a decrease in DNA synthesis and an increase in protein synthesis (Arisaka et al. 1995). The mRNA expressions of exostosin glycosyltransferase-1 and glycosyltransferase-2 (EXT1 and EXT2), two genes encoding glycosyltransferases involved in the chain elongation step of HS

biosynthesis, did not change under shear stress (Koo et al. 2013). The disruption of actin cytoskeleton by cytochalasin D (CD) abolished the additional synthesis of HS on ECs exposed to shear stress for 24 h, indicating that the actin cytoskeleton plays a role in shear-induced HS biosynthesis.

In a recent study, Liu et al. (2016) detected that transcriptional expression of HSPGs (syndecan family and glypican-1) in HUVECs responded to the distinct magnitudes of shear stress. During the initial 0.5 h of exposure, syndecan-1 mRNA was the most upregulated, by 4 dyn/cm^2 of shear stress, and syndecan-4 mRNA was significantly upregulated, by 10 and 15 dyn/cm^2. After 24 h of exposure, the greatest increase in mRNA was syndecan-4 under 4 dyn/cm^2, and syndecan-3 under 15 dyn/cm^2. All the three magnitudes of shear stress (4, 10, and 15 dyn/cm^2) resulted in a significant increase in glypican-1 mRNA after 24 h exposure. Compared with static control, there was a 1.7-, 3.4-, and 4.1-fold increase in glypican-1 mRNA at 24 h under 4, 10, and 15 dyn/cm^2, respectively, but was not significantly changed at 0.5 h (Liu et al. 2016). These molecular changes that may be responsible for dynamic remodeling of the glycocalyx and associated with vascular homeostasis and endothelial dysfunction revealed the potential candidate components of the glycocalyx in response to cardiovascular diseases.

Moreover, increases in sulfated GAGs in the circulation media were detected after 24 h of shear exposure in an earlier study (Arisaka et al. 1995). Although researchers did not observe enhanced sulfated GAGs in the circulation media after 30 min of shear exposure (Zeng et al. 2013), they have not examined this issue at 24 h due to loss of cells from the edges of the cover slide artificially elevating the media concentration of sulfated GAG (Zeng and Tarbell 2014).

5.2 Cytoskeleton and ESG

Many studies of mechanotransduction in endothelial cells are based on the initial exposure of statically cultured cells to a step change in shear stress (Haidekker et al. 2000; Rizzo et al. 2003; Chien 2007; Pahakis et al. 2007; Yao et al. 2007). Shear stress induces EC responses via cytoskeleton-dependent and cytoskeleton - independent pathways (Silver and Siperko 2003; Wang et al. 2008) including the glycocalyx which is an important mechanosensing element on the plasma membrane surface (Tarbell and Pahakis 2006; Wang et al. 2008).

Longer-term adaptation of the endothelium to fluid shear stress is dominated by transformation in the actin cytoskeleton resulting in rearrangement of filamentous actin (F-actin) into bundles of stress fibers aligned in the direction of flow and into a diffuse network of short microfilaments including lamellipodia and filopodia (Gotlieb 1990; Malek and Izumo 1996; Li et al. 2005).The stress fiber bundles are composed of actin filaments in parallel alignment that function as cellular cytoskeletal-contractile elements (Sanger and Sanger 1980; Gotlieb 1990).

In static conditions (no shear stress), prominent microfilament bundles, the dense peripheral bands, are present at the cell periphery of confluent EC monolayers (Sanger and Sanger 1980; Satcher et al. 1997). Shear-induced increases in caveolin-1/caveolae and actin are predominantly distributed in the apical regions of the cell where a sustained clustering of lipid rafts occurs (Zeng and Tarbell 2014). Stress fibers are believed to support caveolae in the apical membrane by their association with caveolin-1 (Thomsen et al. 2002; Navarro et al. 2004). Thus, it appears that the distribution of F-actin over the cell surface, including that which has been newly synthesized, provides a supporting scaffold for new caveolae and their associated glypican/HS. It has been demonstrated that caveolae and caveolin-1 are crucial for both short- and long-term mechanotransduction in blood vessels of mice (Yu et al. 2006). Newly synthesized syndecan supported by actin provides a platform for additional HS and CS that have been synthesized as well. This is summarized in Fig. 8.

The associations of syndecan-1 with stress fiber and lamellipodia protrusion have been indicated in several studies (Carey et al. 1996; Chakravarti et al. 2005; Couchman 2010). In ad-

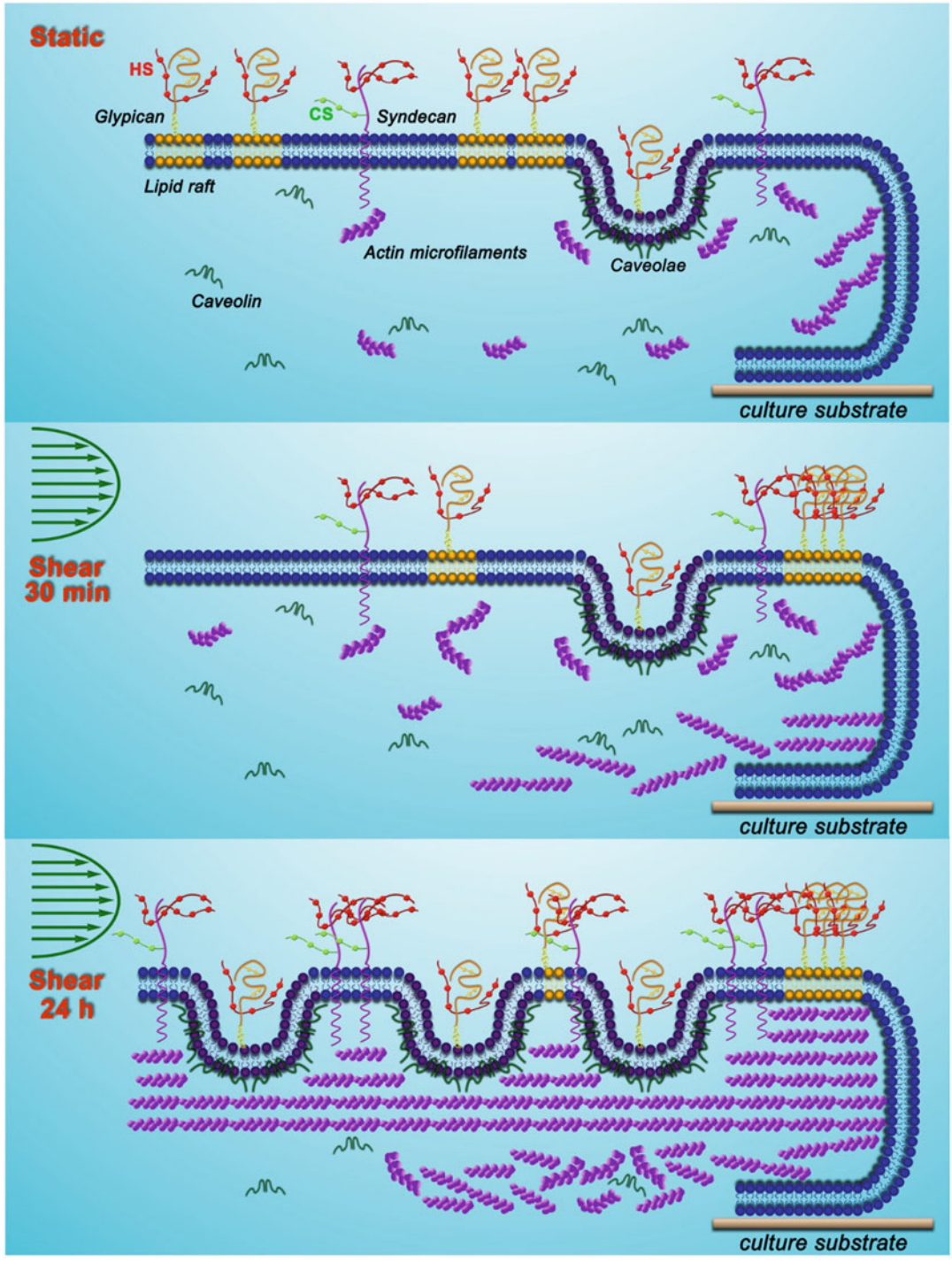

Fig. 8 Adaptive remodeling of glycocalyx with membrane rafts and actin cytoskeleton. Under static conditions, glypican-1 carrying only HS is localized on the dispersed lipid rafts and caveolae on the membrane. The actin cytoskeleton interacts with the transmembrane protein syndecan-1 and the caveolar structural protein caveolin-1 for stabilization. After 30 min of shear exposure, lipid rafts have carried glypican-1 with anchored HS to the cell boundary (clustering), while syndecan-1 carrying HS and CS and caveolae with localized

dition, HS plays a central role in mediating fluid shear stress-induced cell motility and proliferative response (Yao et al. 2007) and change of the actin cytoskeleton (Thi et al. 2004; Moon et al. 2005). To test whether actin cytoskeleton responsible the dynamic remodeling of the glycocalyx, actin cytoskeleton was disrupted by CD (Zeng and Tarbell 2014; Li and Wang 2017). At static conditions (without flow), the glycocalyx was not disrupted after CD treatment. Interestingly, the administration of CD (40 nM) did not prevent the clustering of HS on RFPECs in response to shear stress at 30 min, but abolished the recoverage of HS at 24 h (Zeng and Tarbell 2014). The phenomena at 24 h were also shown on HUVCEs and human aortic endothelial cells (HAECs) by Li and Wang (2017). These results suggested that the shear stress-induced clustering of HS at 30 min is actin cytoskeleton-independent and that the actin cytoskeleton plays an important role in the reorganization of the glycocalyx at 24 h. The dynamic modeling of the glycocalyx might contribute in both cytoskeleton-dependent and cytoskeleton -independent pathways.

5.3 S1P and ESG

S1P is emerging as a potent modulator of endothelial function in response to injury (Sanchez 2016). S1P exerts a variety of biological actions through binding with the specific G-protein-coupled receptors ($S1P_{1–5}$) on the cell surface to activate signaling cascades or serve as a second messenger (Meyer zu Heringdorf and Jakobs 2007). Receptors $S1P_{1–3}$ are expressed in many tissues in the cardiovascular system (Kimura et al. 2000; Kono et al. 2004) and have been widely investigated. S1P and its receptor, $S1P_1$, were required for embryonic angiogenesis and vascular stabilization (Kono et al. 2004). S1P can promote the formation of an actin ring around vascular ECs and strengthen cell-cell and cell-matrix interactions through $S1P_1$, maintaining the low permeability of the vascular wall (Curry and Adamson 2013). The specific agonist of $S1P_1$ (KRP-203) significantly inhibits the formation and development of AS but does not influence the S1P level in plasma (Poti et al. 2013). When mice were fed a high-fat diet, the development of an abnormal vascular phenotype and development of plaque were obvious in the descending aorta in the $Apoe^{-/-}$ and EC-specific $S1P_1$ null mice ($S1P_1^{f/f}$ VE-cadherin-Cre-ER^{T2}), but were not evident in the $Apoe^{-/-}$ and $S1P_1$ wild-type mice (Jung et al. 2012), showing that S1P could maintain the vascular homeostasis and prevent the development of AS through $S1P_1$.

How might the above observations be related to the glycocalyx? The EC glycocalyx was modified/degraded after removal of plasma components, particularly albumin, from the bathing media (Michel et al. 1985). In a recent study, it was demonstrated that S1P carried by albumin inhibits shedding of the syndecan-1 ectodomain on EC via activation of $S1P_1$ receptor (Zeng and Tarbell 2014), and thus maintains the normal vascular permeability in intact microvessels (Sha et al. 2016). The depletion of plasma protein induces syndecan-1 shedding through MMP-mediated proteolytic cleavage close to the plasma membrane on the external face (Zeng and Tarbell 2014). The shedding of the syndecan-1 ectodomain also takes away the attached HS and CS (Zeng and Tarbell 2014). After complete shedding of glycocalyx components (including syndecan-1 with attached HS and CS) by depletion of

Fig. 8 (continued) glypican-1 and anchored HS do not move. Actin microfilaments increase in both apical and basal aspects of the cell. After 24 h of exposure, new caveolae are assembled on the apical surface, which may associate with newly synthesized glypican-1. Syndecan-1 (HS/CS) and glypican-1(HS) that are bound to anchored caveolae and mobile lipid rafts are synthesized and result in nearly uniform distributions of HS and CS. Numerous long stress fibers form and most distribute in the apical part of the cell, where they stabilize new caveolae and syndecan-1. In the basal part of the cell, actin microfilaments increase, scatter, and arrange in a disorderly fashion. Our findings portray a dynamic reorganization of the EC glycocalyx (Cited from Zeng and Tarbell (2014))

plasma protein, the addition of S1P induced the recovery of endothelial glycocalyx via a PI3K pathway (Zeng et al. 2015). It was suggested that the stability of glycocalyx conferred by S1P is at least partially due to the synthesis of glycocalyx components. It can be concluded that S1P maintains the stability of glycocalyx through inhibiting the shedding and promoting the synthesis of glycocalyx components thereby contributing to the maintenance of normal vascular permeability (Sha et al. 2016) and controlling cardiovascular and immune functions (Curry and Adamson 2013). The intracellular signaling pathway involved in the S1P preserved/induced glycocalyx is still not completely understood. The activation of MMPs by inhibition of $S1P_1$ phosphorylation might be mediated by a pathway involving phosphatidylinositide 3-kinase (PI3K)/Akt and Rac1. It was demonstrated that Akt-mediated phosphorylation of $S1P_1$ (T236) is indispensable for S1P-induced Rac activation, endothelial migration, and morphogenesis (Lee et al. 2001). In addition, activation of $S1P_1$ promotes endothelial barrier integrity, migration, and survival through PI3k/Akt, eNOS, and Rac (Dudek et al. 2004; Adyshev et al. 2011). However, the activation of endothelial $S1P_3$ and $S1P_2$ could counteract the anti-inflammatory actions mediated by the $S1P_1$-PI3K/Akt-eNOS pathway.

Furthermore, vascular endothelial $S1P_1$ can respond to hemodynamic force and transduce the signals into a response that promotes the stabilization of newly formed vascular networks (Jung et al. 2012). Knockout of $S1P_1$ gene in mouse manifests as injured vessel maturation and embryonic mortality. In areas of laminar flow with high shear stress, $S1P_1$ is present on the membrane, whereas it is internalized in areas of disturbed flow with low shear stress. $S1P_1$ regulates the directional migration of lymphatic endothelial cells in response to fluid shear stress, which requires plasma or S1P (Surya et al. 2016). The change in $S1P_1$ might be associated with remodeling of the glycocalyx, and this could in turn alter mechanotransduction by the glycocalyx as discussed earlier in this section.

Cantalupo et al. (2017) identified S1P-$S1P_1$-NO signaling as a new regulatory pathway in vivo of vascular relaxation to flow and blood pressure homeostasis, providing a novel therapeutic target for the treatment of hypertension. Further investigations into the mechanoglycobiological mechanisms underlying the remodeling of the glycocalyx could bridge the effects of shear stress and S1P on atherosclerosis.

6 Angiogenesis and ESG

The term "angiogenesis" is commonly used to reference the process of vessel growth but in the strictest sense denotes vessels sprouting from pre-existing ones (Potente et al. 2011). Inadequate angiogenesis causes ischemia in myocardial infarction, stroke, and neurodegenerative or obesity-associated disorders, whereas excessive angiogenesis promotes many ailments including cancer, inflammatory disorders such as atherosclerosis, and eye diseases (Folkman 2007; Potente et al. 2011). The angiogenetic process is rather complex involving localized breakdown of the basement membrane and ECM of a pre-existing vessel, proliferation and migration of capillary EC into surrounding tissue, and new vessel formation. Stimulated by the proangiogenic signals including cytokines and associated receptors, ECs become motile and invasive.

Glycocalyx plays important roles in angiogenesis through its involvement in EC migration, proliferation, and differentiation (Alexopoulou et al. 2007; Tarbell and Cancel 2016). Through HS chains, HSPGs interact with growth factors such as vascular endothelial growth factor (VEGF) and fibroblast growth factors (FGFs) involved in vascular development and repair, extracellular matrix (ECM) components such as fibronectin and vitronectin, and many collagens. It is generally believed that HSPGs act as co-receptors working in concert with other cell surface receptors leading to high affinity binding. Examples are FGF receptors (FGFRs) interacting with FGFs and $\alpha_5\beta_1$ integrin interacting with fi-

bronectin (Steinfeld et al. 1996). Specific HSPGs carry out the functions of co-receptors in angiogenesis as well (Qiao et al. 2003).

VEGFs are mitogens for endothelial cells. There are seven VEGF isoforms which are generated via an alternative splicing mechanism from a unique gene (Achen and Stacker 1998; Neufeld et al. 1999). Among them, $VEGF_{165}$ is a major angiogenic factor that is inactivated by oxidizing agents and free radicals to inhibit angiogenesis (Gitay-Goren et al. 1996). KDR (kinase insert domain-containing receptor)/Flk-1 receptor (VEGFR2) and Flt-1 (VEGFR1) are type III tyrosine kinase receptors that bind to $VEGF_{165}$. Flt-1 with a tenfold higher affinity to VEGF than Flk-1. Flk-1 plays important roles in proliferation, migration, and permeability (Waltenberger et al. 1994; Bernatchez et al. 1999), whereas Flt-1 is responsible for the stabilization of new vascular channel (Fong et al. 1995; Chappell et al. 2016). EC also express $VEGF_{165}$-specific receptors ($VEGF_{165}$Rs, neuropilin-1 and neuropilin-2) via their exon 7 (amino acids 116–159 of $VEGF_{165}$)-encoded domains (Soker et al. 1997). HS is required to bind $VEGF_{165}$ to Flk-1 resulting in retention of $VEGF_{165}$ on the cell surface or in the ECM and for the mitogenic activity of $VEGF_{165}$ (Gitay-Goren et al. 1992; Ono et al. 1999; Stringer 2006; Teran and Nugent 2015). Glypican-1 on EC can interact with $VEGF_{165}$ mediated by the HS chains of glypican-1 and could recuperate the biological activity of $VEGF_{165}$ that was damaged by oxidation (Gengrinovitch et al. 1999). This may be important under conditions including wound repair, hypoxia-induced angiogenesis, or inflammation in which oxidants or free radicals are produced and may damage VEGFs (Gengrinovitch et al. 1999). In recent years, it was shown heparanase derived from myeloma cells activates Flk-1 through shedding of syndecan-1 in human microvascular EC (HMEC-1) thus promoting angiogenesis (Haddad et al. 2015; Jung et al. 2016). Heparanase also regulates syndecan-4 expression (Haddad et al. 2015). However, syndecan-1 coupled insulin-like growth factor-1 receptor (IGF1R) and $\alpha_V\beta_3$ integrin are required for Flk-1 and $\alpha_V\beta_3$-integrin activation during angiogenesis (Rapraeger et al. 2013). The increase in syndecan-1 and decrease in syndecan-4 in HUVECs were involved in low molecular weight fucoidan-induced angiogenesis (Haddad et al. 2015). Syndecan-1 is required in the local tissue environment for angiogenesis (Andersen et al. 2015; Tang and Weitz 2015). Moreover, in glomerular ECs, downregulation of syndecan-1 increased cell permeability, decreased cell viability, and inhibited tube formation through inhibiting VEGF-Flk-1 signaling by recruiting Flk-1 to the caveolin-dependent endocytosis route (Jing et al. 2016). How both shedding of syndecan-1 and upregulation of syndecan-1 could induce angiogenesis has not been completely clarified.

Syndecan-2 and syndecan-3 might also regulate angiogenesis in pathological conditions. Shedding of syndecans occurs in response to stimuli such as inflammatory mediators and growth factors. Shed syndecan-2 regulates angiogenesis by inhibiting EC migration via CD148 (PTPRJ) signaling (De Rossi et al. 2014). Shed syndecan-3 also inhibits angiogenesis by reducing the migratory abilities of ECs (De Rossi and Whiteford 2013).

Basic FGFs (bFGFs) are also potent endothelial growth factors that are capable of inducing angiogenesis (Joseph-Silverstein and Rifkin 1987). Glypican-1 stimulates the biological activity of bFGFs when released by PI-PLC from the surface of endothelial cells (Bashkin et al. 1992). In bovine capillary ECs, bFGF-bound GAGs were degraded by heparinase but not by chondroitinase ABC, suggesting HS bound with bGFG (Saksela and Rifkin 1990). The inclusion of bFGF (10 ng/mL for 16 h) in the culture medium increased release of HSPGs from bovine capillary ECs through increasing plasminogen activity. Pretreatment of cells with TGF-β (4 ng/mL for 6 h) before addition of bFGF inhibited the release of HSPG (Saksela and Rifkin 1990). Overexpression of glypican-1 in normal brain EC enhanced cell growth and sensitized cells to FGF2-induced mitogenesis, while overexpression of syndecan-1 had no effect (Qiao et al. 2003).

In cell recruitment, it is believed that both chemokine oligomerization and binding to GAGs are required. Chemokine interactions with GAGs facilitate the formation of chemokine gradients which provide directional cues for migrating cells (Dyer et al. 2016). A recent study demonstrated that HS is essential for interleukin (IL)-8-induced cell migration (Yan et al. 2016). After enzymatic removal of HS, they observed significant suppression of the IL-8-upregulated Rho GTPases including Cdc42, Rac1, and RhoA (Yan et al. 2016). IL-8-increased Rac1/Rho activity, as well as IL-8-induced polymerization and polarization of actin cytoskeleton and an increase in stress fibers were also suppressed. However, the interplay between the IL-8 receptors and syndecan co-receptors is still not well understood.

In addition, both HS-ligand binding and interactions of PG core proteins with cytoskeletal and/or signaling molecules are required for cell adhesion and migration. Depletion of syndecan-1 (Ebong et al. 2014) and syndecan-4 (Baeyens et al. 2014) have been shown to cause a failure to sense flow direction and inhibition of flow-induced alignment in vitro.

7 Conclusions

In the course of this review, many unanswered questions were raised, and future directions for research were suggested. In this final section, we will highlight several critical areas for future research.

Section 2 discussed composition, organization, and structure of the ESG. It is clear from this section that different methods of observation have produced a model of the ESG consisting of a more rigid inner region on the order of 500 nm in thickness that is detected by biophysical methods including red cell and large tracer molecule exclusion as well as direct physical probing with AFM and a more extended outer region of micron scale that is detected by various forms of light microscopy and cryo-SEM. The inner layer is thought to contain the proteoglycan core proteins and GAGs, while the outer layer is diffuse containing absorbed proteins, charged ions, and additional GAGs. This model requires direct validation by advanced imaging techniques such as STORM and SEM with immuno-labeled nanoparticles.

Section 3 focused on mechanical properties of the ESG. There appears to be consistency in measurements and calculations of the elastic modulus of the inner region of the ESG in the range $E = 0.3–0.7$ kPa that is an order of magnitude lower than the underlying plasma membrane. These measurements should be extended to additional cell types, and the structural components (proteoglycans and GAGs) of the ESG that control this mechanical property should be determined in order to provide a more direct understanding of how mechanical forces are transmitted to cells. It seems unlikely that AFM measurements will be capable of dissecting out the contributions of individual components directly since AFM only has resolution to treat the ESG as a homogeneous layer. Rather, knockdown of individual components followed AFM measurements may be informative. Because the ESG remodels dramatically after exposure to shear stress (Sect. 5), it will be important to extend ESG mechanical property measurements to fully flow adapted cells (after 24 h of shear).

Section 4 considered mechanotransduction and the ESG. In a variety of studies including enzyme treatments, gene knockdown, and direct force application (AFM), glypican-1 has emerged as the proteoglycan core protein that delivers shear force to the cell body for transduction into NO in the sustained phase of production. This is a somewhat controversial conclusion that should be validated in an animal model such as the glypican-1 knockout mouse. The detailed interface between the inner and outer layers of the two-layer model of the ESG that allows fluid shear forces in the outer layer to be transmitted to the proteoglycan core proteins in the inner layer remain to be determined. The intracellular signaling pathway by which mechanical activation of glypican-1 leads to the phosphorylation of PECAM-1 has not been elucidated, and the role of HSPG in the

early phase of NO production requires further investigation.

Section 5 described remodeling of the ESG. Transient remodeling after initial exposure to shear stress involves dramatic movement of glypican-1 toward cell boundaries in lipid rafts before the onset of new synthesis or cytoskeletal remodeling. This early remodeling may be involved in the association of HSPG with Gαq/11-PECAM-1 which mediates early phase mechanotransduction to produce NO, but this has not been determined. Long-term remodeling (24 h) establishes a more uniform distribution of ESG components resembling the in vivo state as a result of new HSPG synthesis and cytoskeletal remodeling. Glypican-1 is distributed in caveolae and at cell junctions in lipid rafts. It is tempting to conclude that mechanotransduction to produce NO is initiated in the lipid rafts, but currently this is not known. In addition, the intracellular signaling mechanisms that mediate new synthesis of ESG components are not established.

Section 6 reviewed angiogenesis and the ESG. The ESG is involved in many mechanisms that contribute to angiogenesis, most notably binding of growth factors on the EC surface and in the ECM which contribute to EC migration, proliferation, and differentiation. The ESG also senses interstitial flow that is known to enhance angiogenesis. However, a coherent picture of ESG involvement in angiogenesis remains to be elucidated.

Finally, we note that recent advances in our understanding of the many roles that the ESG plays in normal physiology and pathophysiology suggest that the structural integrity of ESG that is regulated by physical forces is absolutely central for mechanotransduction, cell proliferation, cell adhesion, and cell migration. Future research in mechanoglycobiology should focus on determining the mechanisms by which physical forces regulate the structure and composition of the ESG with particular emphasis on synthesis and regeneration in the face of pathological changes in structure and function. Such understanding of mechanoglycobiology may facilitate the treatment of many diseases including atherosclerosis, stroke, sepsis, diabetes, hypertension, pulmonary edema, fibrosis, and cancer.

Acknowledgments We would like to acknowledge the support from the National Natural Science Foundation of China [Grant no. 11402153(YZ)], National Institutes of Health [grant nos. SC1CA153325 (BF), RO1HL094889 (JT, BF), and RO1CA204949 (JT)].

References

Achen MG, Stacker SA (1998) The vascular endothelial growth factor family; proteins which guide the development of the vasculature. Int J Exp Pathol 79(5):255–265

Adamson RH, Clough G (1992) Plasma proteins modify the endothelial cell glycocalyx of frog mesenteric microvessels. J Physiol 445:473–486

Adyshev DM, Moldobaeva NK, Elangovan VR, Garcia JG, Dudek SM (2011) Differential involvement of ezrin/radixin/moesin proteins in sphingosine 1-phosphate-induced human pulmonary endothelial cell barrier enhancement. Cell Signal 23(12):2086–2096

Alexopoulou AN, Multhaupt HA, Couchman JR (2007) Syndecans in wound healing, inflammation and vascular biology. Int J Biochem Cell Biol 39(3):505–528

Andersen NF, Kristensen IB, Preiss BS, Christensen JH, Abildgaard N (2015) Upregulation of Syndecan-1 in the bone marrow microenvironment in multiple myeloma is associated with angiogenesis. Eur J Haematol 95(3):211–217

Arisaka T, Mitsumata M, Kawasumi M, Tohjima T, Hirose S, Yoshida Y (1995) Effects of shear stress on glycosaminoglycan synthesis in vascular endothelial cells. Ann N Y Acad Sci 748:543–554

Arkill KP, Knupp C, Michel CC, Neal CR, Qvortrup K, Rostgaard J, Squire JM (2011) Similar endothelial glycocalyx structures in microvessels from a range of mammalian tissues: evidence for a common filtering mechanism? Biophys J 101(5):1046–1056

Arkill KP, Neal CR, Mantell JM, Michel CC, Qvortrup K, Rostgaard J, Bates DO, Knupp C, Squire JM (2012) 3D reconstruction of the glycocalyx structure in mammalian capillaries using electron tomography. Microcirculation 19(4):343–351

Baeyens N, Mulligan-Kehoe MJ, Corti F, Simon DD, Ross TD, Rhodes JM, Wang TZ, Mejean CO, Simons M, Humphrey J, Schwartz MA (2014) Syndecan 4 is required for endothelial alignment in flow and atheroprotective signaling. Proc Natl Acad Sci U S A 111(48):17308–17313

Bai K, Wang W (2012) Spatio-temporal development of the endothelial glycocalyx layer and its mechanical property in vitro. J R Soc Interface 9(74):2290–2298

Baldwin AL, Winlove CP (1984) Effects of perfusate composition on binding of ruthenium red and gold colloid to glycocalyx of rabbit aortic endothelium. The

journal of histochemistry and cytochemistry: official journal of the. Hist Soc 32(3):259–266
Bartosch AMW, Mathews R, Tarbell JM (2017) Endothelial glycocalyx-mediated nitric oxide production in response to selective AFM pulling. Biophys J 113(1):101–108
Bashkin P, Neufeld G, Gitay-Goren H, Vlodavsky I (1992) Release of cell surface-associated basic fibroblast growth factor by glycosylphosphatidylinositol-specific phospholipase C. J Cell Physiol 151(1):126–137
Bernatchez PN, Soker S, Sirois MG (1999) Vascular endothelial growth factor effect on endothelial cell proliferation, migration, and platelet-activating factor synthesis is Flk-1-dependent. J Biol Chem 274(43):31047–31054
Bernfield M, Gotte M, Park PW, Reizes O, Fitzgerald ML, Lincecum J, Zako M (1999) Functions of cell surface heparan sulfate proteoglycans. Annu Rev Biochem 68:729–777
Betteridge KB, Arkill KP, Neal CR, Harper SJ, Foster RR, Satchell SC, Bates DO, Salmon AHJ (2017) Sialic acids regulate microvessel permeability, revealed by novel in vivo studies of endothelial glycocalyx structure and function. J Physiol 595(15):5015–5035
Brands J, Van Teeffelen JWGE, Van den Berg BM, Vink H (2007) Role for glycocalyx perturbation in atherosclerosis development and associated microvascular dysfunction. Futur Lipidol 2(5):527–534
Cai B, Fan J, Zeng M, Zhang L, Fu BM (2012) Adhesion of malignant mammary tumor cells MDA-MB-231 to microvessel wall increases microvascular permeability via degradation of endothelial surface glycocalyx. J Appl Physiol (1985) 113(7):1141–1153
Cantalupo A, Gargiulo A, Dautaj E, Liu C, Zhang Y, Hla T, Di Lorenzo A (2017) S1PR1 (Sphingosine-1-Phosphate Receptor 1) signaling regulates blood flow and pressure. Hypertension 70(2):426–434
Carey DJ, Bendt KM, Stahl RC (1996) The cytoplasmic domain of syndecan-1 is required for cytoskeleton association but not detergent insolubility. Identification of essential cytoplasmic domain residues. J Biol Chem 271(25):15253–15260
Chakravarti R, Sapountzi V, Adams JC (2005) Functional role of syndecan-1 cytoplasmic V region in lamellipodial spreading, actin bundling, and cell migration. Mol Biol Cell 16(8):3678–3691
Chappell JC, Cluceru JG, Nesmith JE, Mouillesseaux KP, Bradley VB, Hartland CM, Hashambhoy-Ramsay YL, Walpole J, Peirce SM, Mac Gabhann F, Bautch VL (2016) Flt-1 (VEGFR-1) coordinates discrete stages of blood vessel formation. Cardiovasc Res 111(1):84–93
Chien S (2007) Mechanotransduction and endothelial cell homeostasis: the wisdom of the cell. Am J Physiol Heart Circ Physiol 292(3):H1209–H1224
Conway DE, Breckenridge MT, Hinde E, Gratton E, Chen CS, Schwartz MA (2013) Fluid shear stress on endothelial cells modulates mechanical tension across VE-cadherin and PECAM-1. Curr Biol 23(11):1024–1030
Couchman JR (2010) Transmembrane signaling proteoglycans. Annu Rev Cell Dev Biol 26:89–114
Curry FE, Adamson RH (2012) Endothelial glycocalyx: permeability barrier and mechanosensor. Ann Biomed Eng 40(4):828–839
Curry FR, Adamson RH (2013) Tonic regulation of vascular permeability. Acta Physiol (Oxf) 207(4):628–649
Dabagh M, Jalali P, Butler PJ, Randles A, Tarbell JM (2017) Mechanotransmission in endothelial cells subjected to oscillatory and multi-directional shear flow. J R Soc Interface 14(130):pii: 20170185
Davies PF (2009) Hemodynamic shear stress and the endothelium in cardiovascular pathophysiology. Nat Clin Pract Cardiovasc Med 6(1):16–26
Davies PF, Dewey CF Jr, Bussolari SR, Gordon EJ, Gimbrone MA Jr (1984) Influence of hemodynamic forces on vascular endothelial function. In vitro studies of shear stress and pinocytosis in bovine aortic cells. J Clin Invest 73(4):1121–1129
De Haan L, Hirst TR (2004) Cholera toxin: a paradigm for multi-functional engagement of cellular mechanisms (review). Mol Membr Biol 21(2):77–92
De Rossi G, Whiteford JR (2013) A novel role for syndecan-3 in angiogenesis. F1000 Res 2:270
De Rossi G, Evans AR, Kay E, Woodfin A, McKay TR, Nourshargh S, Whiteford JR (2014) Shed syndecan-2 inhibits angiogenesis. J Cell Sci 127(Pt 21):4788–4799
Deepa SS, Yamada S, Zako M, Goldberger O, Sugahara K (2004) Chondroitin sulfate chains on syndecan-1 and syndecan-4 from normal murine mammary gland epithelial cells are structurally and functionally distinct and cooperate with heparan sulfate chains to bind growth factors. A novel function to control binding of midkine, pleiotrophin, and basic fibroblast growth factor. J Biol Chem 279(36):37368–37376
van den Berg BM, Vink H, Spaan JA (2003) The endothelial glycocalyx protects against myocardial edema. Circ Res 92(6):592–594
van den Berg BM, Spaan JA, Vink H (2009) Impaired glycocalyx barrier properties contribute to enhanced intimal low-density lipoprotein accumulation at the carotid artery bifurcation in mice. Pflugers Arch 457(6):1199–1206
Dudek SM, Jacobson JR, Chiang ET, Birukov KG, Wang P, Zhan X, Garcia JG (2004) Pulmonary endothelial cell barrier enhancement by sphingosine 1-phosphate: roles for cortactin and myosin light chain kinase. J Biol Chem 279(23):24692–24700
Dyer DP, Salanga CL, Volkman BF, Kawamura T, Handel TM (2016) The dependence of chemokine-glycosaminoglycan interactions on chemokine oligomerization. Glycobiology 26(3):312–326
Ebong EE, Macaluso FP, Spray DC, Tarbell JM (2011) Imaging the endothelial glycocalyx in vitro by rapid freezing/freeze substitution transmission electron microscopy. Arterioscler Thromb Vasc Biol 31(8):1908–1915
Ebong EE, Lopez-Quintero SV, Rizzo V, Spray DC, Tarbell JM (2014) Shear-induced endothelial NOS acti-